Vacuum and excited states of Coulomb-gauge SU(n) Yang-Mills fields

R. E. Cutkosky and K. C. Wang
Physics Department, Carnegie-Mellon University, Pittsburgh, Pennsylvania 15213
(Received 30 November 1987)

Properties of the quantized SU(n) Yang-Mills fields, for $n=2$, 3, and 4, have been studied numerically. We apply the Hamiltonian formalism to the continuum theory, with a truncated momentum expansion in a finite volume, and have examined states in the vacuum sector using variational methods in the Coulomb gauge. The results depend on the strength of the interaction constant α, with a transition at $n\alpha \sim 1$. For small α, there is a gap between excited-state energies and the vacuum energy, but the excited 0^{++} states correspond to pairs of weakly interacting transverse gluons. For larger α, the excited states are associated with a collective degree of freedom and can be identified with a glueball. There is no evidence for the existence of an instability associated with magnetic interactions.

I. INTRODUCTION

The central problem of strong-interaction physics is to understand how the confinement mechanism of QCD operates, and how it produces the observed properties of physical particles. Many interesting results have already been obtained by Monte Carlo simulation of lattice gauge theories, but it is also useful to investigate other approaches, which can give complementary insights and might eventually even be able to compete in numerical precision. Our nonperturbative, numerical calculations use the Hamiltonian formalism, which allows us to look at the vacuum and low-lying excited states directly. Since our work is based on the continuum theory, inclusion of fermions would give no fundamental complications, but our present numerical calculations have been restricted to pure-glue theories.

We use standard mathematical techniques and approximation methods. The fields are represented by normal-mode expansions in a finite volume. These expansions are truncated at a finite momentum index Λ, giving a quantum system with a finite number of degrees of freedom. The Coulomb gauge is used. This means that constraints can be eliminated and there are no residual unphysical variables. In the inner Gribov[1] domain where the Faddeev-Popov determinant has no zeros, the Hilbert space as well as the Hamiltonian is positive definite. This allows practical use of variational methods.

Gribov pointed out that the properties of the Coulomb-gauge Faddeev-Popov determinant can explain in a simple way the origin of a mass gap in the spectrum of physical states.[1] To examine this scenario for confinement, a sequence of numerical studies were carried out by Cutkosky; the earliest of these used simplified models to illustrate the influence of the determinant.[2] A recent variational calculation has included, for SU(2), the Coulomb energy term in the Hamiltonian.[3] Similar results have been obtained in SU(2) Coulomb-gauge calculations by Schütte and co-workers[4] using cluster-expansion techniques, and the Coulomb energy has been treated perturbatively by Swift and Morrero Rodriguez.[5] We consider here the more physically relevant case of SU(3), with some improvements and corrections. For comparison, we extend the published[3] SU(2) results using the same methods, and we have also examined SU(4), in order to develop insight into large-n approximations.

If the transverse amplitudes become large enough, at the Gribov horizon, the Gauss-law constraint operator[6] Δ (defined below) develops a zero eigenvalue, and the Coulomb energy diverges if the color-charge density σ is nonzero. The amplitudes are thereby constrained, even classically, to lie within the region where Δ has a positive spectrum. The previously reported numerical calculations show that this constraint on the transverse amplitudes is particularly important for long-wavelength components of the gluon field, and effectively prevents them from propagating when $\alpha=g^2/4\pi$ is big enough. As a result, the effective frequencies Ω of the transverse modes have a characteristic dispersion relation of the form suggested by Gribov, in which the minimum frequency ω is higher than the minimum free-field frequency, and occurs at a nonzero momentum. This provides a simple explanation for the existence of a mass gap in the physical spectrum, but somewhat more is needed to ensure that gluons are actually confined. In our calculations, this occurs when gluon self-energies become so large that configurations with local color-charge cancellation are favored. Collective excitations involving these special configurations can still have relatively low energies, but the density of these lower-energy states is greatly reduced. We find that when g becomes large enough, the first excited 0^{++} state does become a locally colorless object. In this regime, there is also a gap between the energy of this state and the energies of the higher excited states, which can be identified with pairs of such particles. These results would be compatible with the phenomenology given by semiclassical "dual superconductor" models of the QCD vacuum.[7-9] However, our calculations do not support suggestions that the dielectric properties of the QCD vacuum might be associated with a magnetic instability.[10-13]

A special feature of our calculations is that we use as a

quantization volume the maximally symmetric simply connected finite domain S^3 (the surface of a four-dimensional sphere). The simply connected topology is especially desirable for the treatment of gauge theories. The symmetry group of S^3 is $O(4)=SU(2)\times SU(2)$, which has just as many parameters as the symmetry group of Euclidean space, and provides rotational invariance as well as a simulation of translational invariance. Note that a periodic cube (hypertorus) with the same circumference as a hypersphere has a volume which is 4π times larger. As a result, we expect that for truncation effects of similar magnitude, the number of modes needed on the hypersphere can be reduced by a factor of about 4π.

On S^3, there are curvature effects to be considered. In a free-field theory, curvature corrections to the spectrum can be calculated explicitly and removed. However, since there is no explicit Lorentz invariance, interactions might lead to corrections in states with different momenta which differ from the corrections for noninteracting particles. Similar boost effects would also occur in the periodic cube, where they may be even more important because they could depend on the direction as well as on the magnitude of the momentum. These boost effects should be studied in further explicit calculations; for the scalar field with a ϕ^4 interaction term (which is similar to a free-field theory) the corrections were found to be unimportant.[14] For electrically charged particles interacting with an external magnetic field, we found that we could minimize the curvature corrections by adjusting parameters.[15] An effect arising from the curvature which might influence scaling properties is that a hadron of given volume on the hypersphere has a smaller surface area than in flat space. As a result, we can expect to estimate volume contributions to the energies of hadrons more reliably than we can estimate surface energies. Along with the breaking of Lorentz invariance, the influence of our regularization methods on gauge invariance should be examined further.

II. HAMILTONIAN

Bosonic modes on the hypersphere S^3 can be efficiently classified by use of the multiplets $(\frac{1}{2}(K+h), \frac{1}{2}(K-h))$ of $SU(2)\times SU(2)$, where the index K labels the total momentum and h is the helicity.[16] The independent dynamical variables are the expansion coefficients q_{Kk} of the transverse-vector potential $\mathbf{A}$, where the label k indicates the color, direction of momentum, and helicity $h=\pm 1$ of a transverse-vector mode; we use the representation in which the q's are diagonal. The color-charge density σ and the scalar potential Φ are auxiliary quantities which are expanded in scalar modes, for which we also use the labels (Kk) except that $h=0$. The expansions in scalar and vector modes are truncated at the same value Λ. The only zero-mode on the hypersphere is the scalar mode with $K=0$, and this is decoupled in states with no net color charge. As a result, S^3 provides a natural infrared regularization which is free of topological complications.

The energy of a free-field transverse mode is $W_K=K+1$. In general, it seems more accurate to identify $K+1$ as the momentum, rather than K. The high-momentum form of matrix elements is then closer to the flat-space limit, giving better scaling behavior. It is also suggested by the motion of charged particles in a magnetic field.[15]

In the Coulomb gauge, $\nabla\cdot\mathbf{A}=0$, the Hamiltonian is[6]

$$H=\tfrac{1}{2}\int dv(E^2+\epsilon^2+B^2)\ , \tag{1}$$

where $\mathbf{E}$ is the transverse part of the electric field, ϵ is the longitudinal part, and the magnetic field is $\mathbf{B}=\nabla\times\mathbf{A}-\frac{1}{2}g\,\mathbf{A}\times\mathbf{A}$. Color indices, the structure constants, and the Faddeev-Popov determinant $F(A)$ have been suppressed from the notation. The expansion coefficients for $\mathbf{E}$ are $-p_{Kk}$, where the p's are conjugate to the q's, and ϵ is defined below. The expansion for the term $\hat{\mathbf{B}}=-\frac{1}{2}g\,\mathbf{A}\times\mathbf{A}$ in the magnetic field involves both transverse and longitudinal modes. We remind the reader that $F(A)$ appears as a weighting function when matrix elements of H are evaluated, and that the correct ordering is $E^2\rightarrow EFE$ and $\epsilon^2\rightarrow\epsilon F\epsilon$.

For our numerical work, we find it convenient to insert a factor $\Gamma=(-\nabla^2)^{-1/2}$ into the color-charge density σ:

$$\sigma=g\Gamma\,\mathbf{A}\cdot\mathbf{E}\ , \tag{2}$$

and $\frac{1}{2}\sigma^2$ then represents a free-field energy density. We also remove Γ from the scalar potential Φ, so that the constraint equation for Φ is

$$\Delta\Phi=(1-g\Gamma\,\mathbf{A}\cdot\nabla\Gamma)\Phi=\sigma\ , \tag{3}$$

where Δ and Γ, as well as $\mathbf{A}\cdot\nabla$, are matrices in the space of scalar modes. The longitudinal electric field is then $\epsilon=-\nabla\Gamma\Phi$, and $\epsilon^2=\Phi^2$. The Faddeev-Popov determinant is $F=\det[\Delta]$.

As in previous work, we make some approximations which simplify the numerical treatment. These include replacement of the actual Gribov horizon by a smoothed-out approximation, use of a class of trial wave functions with restricted correlations between different modes, and an approximate treatment of the non-Abelian magnetic energy contributions. By introducing these approximations, we in effect replace the actual QCD Hamiltonian by a somewhat simplified model Hamiltonian which we expect to have a similar spectrum.

III. CALCULATIONS

The numerical calculations were carried out in two stages. In the "Coulomb" stage, for an appropriate set of values of q_{Kk}, we determined parametrized forms for the inverse of the matrix Δ and for the determinant F. The second stage was a variational calculation for the energies, using these parametrized operators and a polyspherical approximation for the wave functions: $\Psi=\Psi(X_1,\ldots,X_\Lambda)$, where $X_K=\sum_k q_{Kk}^2$. This is a plausible ansatz for the vacuum sector, because the determinant F has approximately this form. Using such trial wave functions, the variational calculations were done in two steps, following the method used by Cutkosky for SU(2), but with some minor generalizations to improve convergence. First, in a "vacuum" step, we determined a first approximation Ψ_0 for the vacuum state, using a trial

wave function which was similar to the usual Gaussian approximation. Then, in a second "excitation" step, Ψ_0 was fixed, and a set of orthogonal functions of the form $\Psi = Q(X)\Psi_0$ was used to improve the energy of the vacuum and to estimate energies of excited states with vacuum quantum numbers. Here $Q(X)$ is a polynomial of maximum degree 5, with $(\Lambda+1)(2\Lambda+1)$ independent terms.

When the fields are expanded in normal modes, $\mathbf{A}\cdot\mathbf{E}$, $\mathbf{A}\times\mathbf{A}$, and the matrix elements of $\mathbf{A}\cdot\nabla$ involve products of the structure constants multiplied by integrals over three-vector or -scalar normal-mode functions. These integrals can be expressed as a product of two 3-j symbols and a reduced matrix element.[16] For use in the "Coulomb" calculations, we constructed tables of these matrix elements, in which the products of the common 3-j symbols were transformed to a real basis.

Since we have already reported on the methods and some of the results of the Coulomb stage of calculation,[17] we shall only give a brief review of the technique and describe some points which are important for the subsequent variational calculations. We used a method developed by Balduz, Cutkosky, and Tsao[18] to determine F and the locus of the horizon. We examine the matrix $D = g\Gamma\,\mathbf{A}\cdot\nabla\Gamma$ for a selected set of amplitude coefficients q_{Kk} chosen in the following way. The ratios of the X_K were kept fixed at the ratios obtained in the previous SU(2) calculation for $\alpha\sim 0.75$, where $\alpha = g^2/4\pi$. The results are not sensitive to the ratios of the X_K; we used a relatively large value for α to fix the ratios, because this seemed to be an interesting region, and also because the matrix is less important for smaller α. For each K, random directions in the K subspace were then chosen, to define the relative values of the q_{Kk}. A sample of 128 different q_{Kk} was selected for each Λ. We then used the Lanczos iteration method to find about 7–15 leading eigenvalues of D of each sign, and the corresponding eigenvectors. The leading eigenvalues of each sign establish the distance to the horizon from the chosen point in the q space for an arbitrary value of α, in each of the two opposite directions from the origin. Using perturbation theory with the leading eigenvectors, we also determine the tangents to the horizon surface at the 256 intersections. As in previous work, we find that the horizon surface can be reasonably well approximated by the ellipsoidal surface $z(q)=1$, where $z(q)=\sum \xi_K q_{Kk}^2$. For the gauge group SU(n), as we reported earlier,[17] we can exhibit the main dependence on n and K by using the formula

$$\xi_K = \frac{n\alpha}{n^2-1}\,\frac{U_K}{2K(K+2)}\,, \tag{4}$$

in which the denominator is the total number $M_K=(n^2-1)N_K$ [with $N_K=2K(K+2)$] of transverse modes with total momentum K. The calculated values of the U_K have been found to be nearly constant, which means that the ξ_K decrease rapidly as K increases. As remarked in the Introduction, this implies that the amplitudes q_{Kk}, for long-wavelength components of the gluon field, will be greatly reduced when α is big enough. For small K, the U_K increase somewhat with n, while for $K\sim\Lambda$ they are nearly constant.

The average value of the relative spacing $t=z_1-z_0$ between the leading zero (at $z_0=1$) and the next-leading zero, for different n and Λ, is shown in Fig. 1. This relative spacing depends primarily on the total number of scalar modes N_E, and is roughly proportional to Λ^{-1}. The degree of smoothness of the horizon is indicated by the quantity s, which is the rms error in the quadratic approximation; as we expect, s is somewhat less than t. Figure 1 also shows, for comparison, the mean value $r=1-\langle z\rangle$ in the vacuum state, as obtained in the final calculations when $n\alpha=1.2$. Since r is about $4s$, replacing z by a smoothed-out function is probably good enough for the vacuum state, but may not be adequate for some of the higher excited states.

Along with the leading eigenvalues of D, we calculated $\mathrm{Tr}D^2$ and $\mathrm{Tr}D^3$; these quantities were used to construct the interpolation formula for the Faddeev-Popov determinant F, as described by Balduz, Cutkosky, and Tsao. We find that F can be adequately approximated as a function of $z(q)$.

The Coulomb energy operator Φ^2 has a number of special properties, which determine its influence on the eigenstates of the Hamiltonian and also affect the way in which we calculate and parametrize it. Since it is a sum of squared terms, it is non-negative. However, the structure of the gluon color-charge operator σ does allow it to vanish. If the parallel components of $\mathbf{A}$ and $\mathbf{E}$ are symmetric in color, there is no contribution to σ, because the color indices are combined using the structure constants. When the fields $\mathbf{A}$ and $\mathbf{E}$ are expanded in modes, the charge-density operator for a given scalar mode can be written as $\sigma = g\sum Y_{Mm,Nn}q_{Mm}p_{Nn}$. Here the Y's are the numerical coefficients described above, given by a spatial integral involving the dot product of the two vector har-

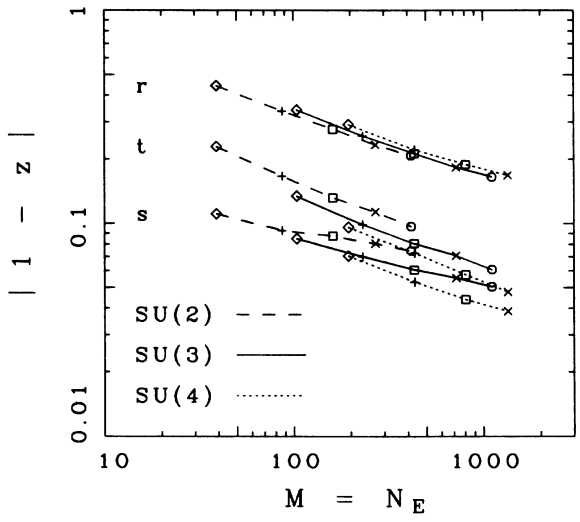

FIG. 1. Properties of the leading zeros of F. Here s gives the rms deviation of the true horizon distance (squared) from the smoothed-out approximation, and $t=z_1-1$ gives the separation of the next zero of the determinant. The quantity r gives, for comparison, the mean value of $1-z$ in the vacuum state for $n\alpha=1.2$.

monic functions (symmetric in the momentum indices) multiplied by the antisymmetric structure constants. Therefore, $Y_{Mm,Nn}$ is an antisymmetric quantity. For matrix elements between wave functions which have the polyspherical form, the replacement $p_{Nn} \to 2q_{Nn}P_N$ can be made, where P_N is conjugate to X_N. The charge operator can therefore be expressed, after summing over m and n, as $\sigma \equiv \sum_{MN} \rho_{MN} P_N$, where ρ_{MN} is antisymmetric. The gluon Coulomb energy can then be written as $\Phi^2 = \sum_{KN} P_K G_{KN} P_N$, where the matrix G satisfies the identity $\sum_N G_{KN} = 0$ as a consequence of the antisymmetry of ρ.

One consequence of this identity is that certain combinations of derivatives of Ψ will not contribute to the Coulomb energy. As we mentioned in the Introduction, this implies that there will be a collective degree of freedom which does not carry color charges, and that excitations associated with this degree of freedom can have relatively low energies.

To calculate the matrix elements G_{KN}, we first need to evaluate

$$\phi_N = \Delta^{-1} \sum_M \rho_{MN} \ . \tag{5}$$

However, in order to get some diagnostic information about the spatial distribution of charges, we also evaluated the auxiliary quantities

$$\phi_N^{LK} = \Pi^L \Delta^{-1} \Pi^K \sum_M \rho_{MN} \ , \tag{6}$$

where Π^K is a projection operator onto scalar modes with total momentum K. We only need to calculate for $N = 1, \ldots, \Lambda - 1$, because we can use the identity to determine the values for $N = \Lambda$.

To determine the ϕ_N^{LK} for each of the ensemble of rays in the space of the q's, we calculate, for several values of z, the inverse of Δ [as multiplying $\Lambda(\Lambda-1)$ different vectors] by the conjugate-gradient method. We chose, for each Λ, three matching points z_j spanning the region of z which had been relevant to the confined regime in the earlier SU(2) calculation. To start off the conjugate-gradient iterations, we use an estimate based on all the calculated eigenvectors and eigenvalues, the known term which is linear in g, and also the inverse as obtained for the next smaller z_j.

Our formula for G_{KN} involves an interpolation in z, and also an extension to other values for the ratios of the X_K. Our prescription is as follows: We first define the auxiliary quantities

$$F_{KN} = \frac{C_{KN}^1}{1-0.7z} + \frac{C_{KN}^2}{1-0.9z} + \frac{C_{KN}^3}{1-z} + \frac{4\tau}{(1-z)^2} \ , \tag{7}$$

where τ is obtained from the leading eigenvector of D, and the C_{KN}^i are chosen to reproduce the value of G_{KN} at the three matching points. Then we write

$$\begin{aligned} G_{KN} &= (f_{KN} + zF_{KN}) X_K X_N \quad \text{for } K \neq N \ , \\ G_{KK} &= -\sum_{N \neq K} G_{KN} \ , \end{aligned} \tag{8}$$

where f_{KN} is the second-order perturbation theory term. This prescription for the dependence on the X's is exact for the term involving f_{KN}, and is an approximation for the remainder.

To construct the magnetic Hamiltonian term $\hat{H} = \frac{1}{2} \int dv \, \hat{\mathbf{B}}^2$, we truncate the expansions for $\hat{\mathbf{B}}$ at the same momentum index $L = \Lambda$ used for other quantities. Somewhat simpler formulas are obtained, however, if we only use the implicit cutoff given by addition of angular momenta, which allows a smoother truncation extending up to $L \sim 2\Lambda$. We shall first describe our treatment of $\hat{H}$ using this simplified version. Expanding the A's in vector modes, we have, explicitly,

$$\begin{aligned} \hat{H} = \tfrac{1}{8} g^2 \sum g_I^i q_J^j q_K^k q_L^l f^{ija} f^{kla} \\ \times \int dv (\mathbf{V}_I^i \times \mathbf{V}_J^j) \cdot (\mathbf{V}_K^k \times V_L^l) \ , \end{aligned} \tag{9}$$

where the f's are the structure constants. To minimize further proliferation of indices, we adopt the convention that the meaning and range of an index such as k depends on the context; that is, on f it refers to the color variable, while on V it labels the spatial mode. The vector-harmonic functions have been normalized so that

$$\int dv \, \mathbf{V}_I^i \cdot \mathbf{V}_J^j = \delta_{IJ} \delta^{ij} \quad \text{and} \quad \sum_k V_K^{kr} V_K^{ks} = \frac{N_K \delta^{rs}}{6\pi^2} \tag{10}$$

(where r and s label the vector components). For polyspherical states, averaging over the q's with fixed X's, we have

$$\langle q_I^i q_J^j q_K^k q_L^l \rangle = \delta_{IK} \delta^{ik} \delta_{JL} \delta^{jl} \frac{X_I X_J}{M_I M_J} Q_{IJ} + \text{interchanges} \ , \tag{11}$$

where $Q_{IJ} = 1$, if $I \neq J$, and $Q_{II} = M_I/(M_I+2)$. Using the value of the Casimir operator along with Eqs. (10) and (11), we obtain

$$\hat{H} = \frac{g^2 n}{12\pi^2 (n^2-1)} \sum_{I,J} X_I X_J Q_{IJ} \ . \tag{12}$$

The effect of truncating the $\hat{\mathbf{B}}$ expansions at Λ is just to insert an extra factor T_{IJ} into the summation in (12), where T_{IJ} is given by a sum over reduced matrix elements. Note that $T_{IJ} = 1$ if $I + J < \Lambda$.

The magnetic Hamiltonian term which is cubic in $\mathbf{A}$ has a vanishing expectation value if the wave function has a polyspherical form. However, this term gives a large negative contribution to the vacuum energy in second-order perturbation theory, and it should not be omitted.[19,4] We use a self-energy approximation (SEA) to include the second-order contribution of this cubic term. For consistency, the quartic magnetic term is then treated in the same way. The SEA magnetic energy is defined to be

$$H_{\text{SEA}} = \sum (\tfrac{1}{2} W_K^2 + \alpha S_K) X_K + \alpha U_0 \ , \tag{13}$$

where $W_K = K + 1$ gives the free-field part of the energy. We choose S_K so that the order-α magnetic contribution to the $\langle$perturbative-vacuum$|$ $|$two-gluon$\rangle$ matrix element will be reproduced. Since S_K by itself will not ex-

actly reproduce the magnetic energy of the vacuum to this order, a constant U_0 has been added, but this term does not contribute to excitation energies. The same idea was used in Cutkosky's SU(2) calculation,[3] but there was a numerical error in the S_K used in that paper. To illustrate the method, we describe how a term $\hat{S}_K$ is derived from (12). In the free-gluon vacuum $|0\rangle$, we have $\langle X_K\rangle = M_K/2W_K$. The excited state is proportional to $(X_K - \langle X_K\rangle)|0\rangle$. Using the matrix elements

$$\langle 0|Q_{IJ}X_IX_J(X_K-\langle X_K\rangle)|0\rangle = (\delta_{IK}+\delta_{JK})\langle X_I\rangle\langle X_J\rangle/W_K\ , \tag{14}$$

$$\langle 0|X_I(X_K-\langle X_K\rangle)|0\rangle = \delta_{IK}\langle X_I\rangle/W_K\ ,$$

we obtain

$$\hat{S}_K = \sum_L \frac{nL(L+2)T_{KL}}{3\pi W_L}\ . \tag{15}$$

The remaining part of S_K is somewhat more complicated, because there is an extra factor X_L as well as the energy denominator $(W_I+W_J+W_L)$. The final corrected values for S_K are shown in Fig. 2; there is an almost complete cancellation between the attractive and repulsive terms, leaving a small net attraction. In the confined regime, the calculated excitation energies were changed very little by correction of the error. Figure 3 compares the results of test calculations for SU(2) in which the SEA term was omitted with our final results in which it is included. In the SEA approximation, the non-Abelian magnetic field term has an insignificant effect on the excitation levels.

For the "vacuum step" of the variational calculations, we use the trial wave function

$$\Psi_0 = (1-z)^2\exp\left[-\tfrac{1}{2}\sum \eta_K X_K + \eta_0 z^2\right]\ , \tag{16}$$

which has $\Lambda+1$ adjustable parameters η_K. This expression is similar to the usual Gaussian approximation, but the Gaussian has been modified by the extra functions of z as well as by the need to weight with F. The quadratic behavior in $1-z$ near $z=1$ is imposed by the structure of the Coulomb energy operator. The use of Gaussian wave functions is common in variational calculations because they often lead to integrals which can be evaluated in closed form. Here, however, we have numerical integrals, because F and the Coulomb energy operator lead to integrals which cannot be evaluated analytically. One reason we use Gaussian-type wave functions is that the derivatives with respect to the parameters η_K and the matrix elements in the basis set obtained by multiplying Ψ_0 by the polynomial $Q(X)$ can be evaluated using similar computer codes. In addition, we know that Eq. (16) will give a good approximation for the larger values of K, even when α is large, because for large K, the dependence of z on the amplitudes will be very weak, and there will be very little deviation from the Gaussian approximation. For the polynomial $Q(X)$, we use all quadratic polynomials in the X_K, and the additional independent polynomials obtained by multiplying these by a polynomial in z of degree $L_Q=3$. In the previous SU(2) calculation,[3] in which the parameter η_0 in Eq. (16) was not used, and L_Q had a maximum value of 2, convergence as L_Q was in-

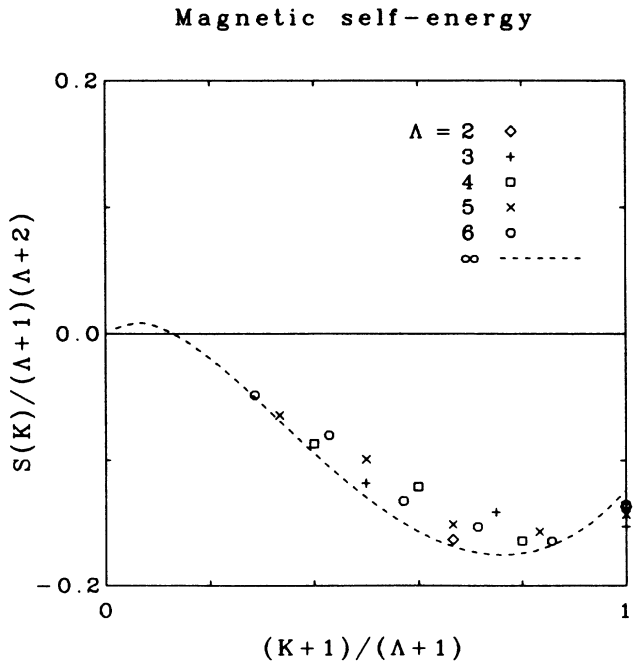

FIG. 2. Values of S_K, our estimate for the higher-order magnetic terms in the SEA Hamiltonian.

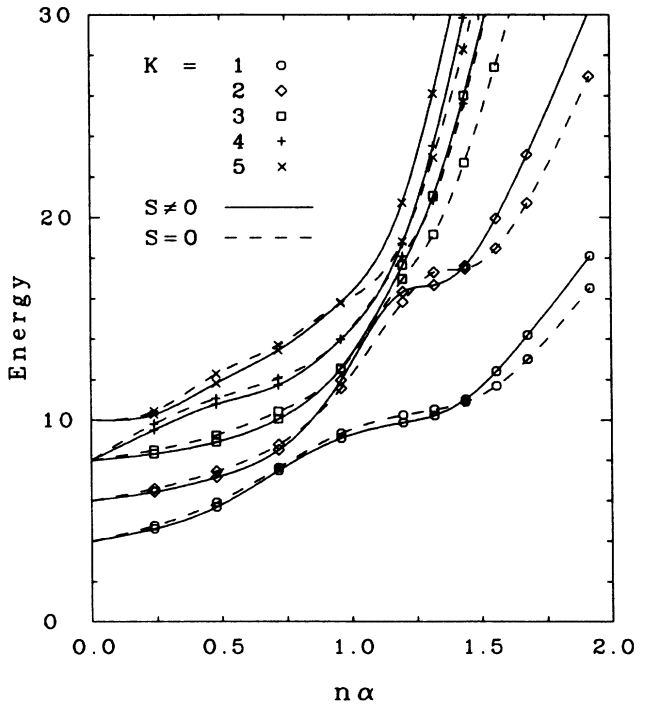

FIG. 3. A comparison, for SU(2) and $\Lambda=5$, of excitation energies as calculated with the term S_K included (solid curves) and with S_K omitted (dashed curves). The plotting symbols show the values of $n\alpha$ for which calculations were made; the connecting curves are spline interpolations.

creased seemed somewhat marginal for the excited states when α was large. The extra parameters used here give Ψ adequate flexibility in the region near the Gribov horizon.

We used a special method for the numerical integrations. For the fixed-z hyperplanes in the space of the X's, an open hexagonal lattice was found to give reliable results. About 10^5 points were used for $\Lambda=6$, with the size of the integrand being checked, roughly, at about 10 times as many points. To integrate over z, we used a mapping which somewhat enlarged the region near $z=1$, with about 50–100 points in the interval $0\le z\le 1$. We also used formulas with weights which had been tuned for the various terms in the Hamiltonian near $z=1$. A difficulty with this method is that it is not so well suited to the free-field limit, where $\langle z\rangle$ is small, especially when n and Λ are large. In this case, Ψ^2 is almost a δ function, located in the region for which the integration was not optimized.

The numerical calculations were carried out on the Cray X-MP at the Pittsburgh Supercomputing Center. In the Coulomb calculations, the computer time was mainly needed for the eigenvalue determination and for the matrix inversion; it depended strongly on the total number of scalar modes N_E, and therefore on n and Λ. For SU(4), we considered only $\Lambda\le 5$. In the variational calculations, extensive computer time was needed for numerical evaluation of the matrix elements of the Hamiltonian; it was very strongly dependent on Λ. Also, we did need to use more integration points for each Λ when n was larger. For SU(3), the two stages of calculation used about equal amounts of computer time.

IV. RESULTS

Figure 4 shows how the wave function for the vacuum state is influenced by the value of α. We plot $\langle\Psi^2\rangle$ for SU(3), for fixed z and integrated over all other variables, against $z/n\alpha$. The density is extremely small when z is small, because it contains a factor $z^{\nu-1}$, where 2ν is the total number of vector modes included in the calculation. For $\alpha=0.24$, the horizon is off-scale and the density is essentially given by the free-field wave function. For $\alpha=0.48$, the location of the horizon is indicated by the $\times$ on the axis. For this value of α, the horizon lies in a region where the free-field wave functions would be large, and the actual wave functions are strongly affected by the presence of the horizon. We see clearly, from Fig. 4, that the probability density does go to zero as the horizon is approached.

To examine how the constraining influence of the horizon affects gluon frequencies, we define effective frequencies Ω_K by $\langle q_{Kk}^2\rangle = R/2\Omega_K$. The "renormalization factor" R was estimated by fitting the calculated values of $\langle q_{Kk}^2\rangle$ with the interpolation formula

$$\Omega_K^2 = W_K^2+\mu(\Lambda+1)^2+\kappa^4/W_K^2 \ , \tag{17}$$

using R, μ, and κ as parameters. We required μ to be independent of Λ. This scaling assumption is actually a good approximation, and allows us to include the value $\Lambda=2$. For SU(3), with $\alpha=0.48$, the $\Omega_K=R/(2\langle q_{Kk}^2\rangle)$ are shown on the left side of Fig. 5. The dots show the

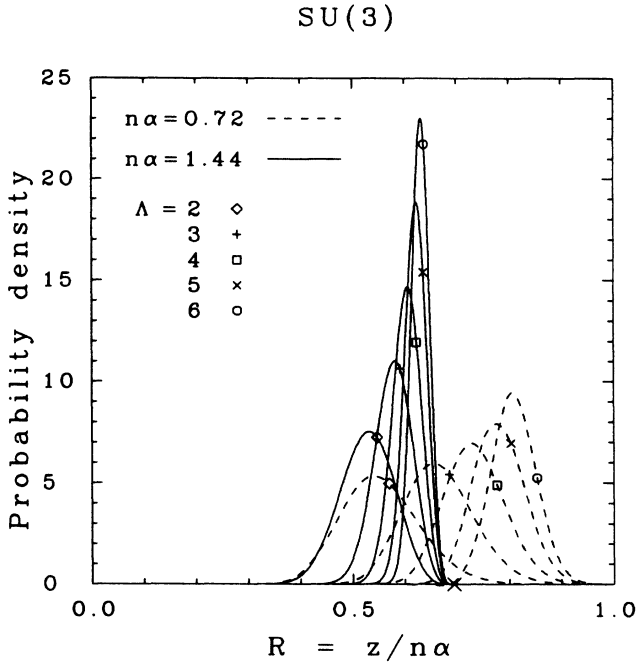

FIG. 4. The density distribution $\langle\Psi^2\rangle$ plotted against $z/n\alpha$, in the unconfined (dashed curves) and confined (solid curves) regimes, for SU(3).

interpolated minima, which define characteristic momenta κ and characteristic frequencies ω. The inverse of the characteristic momentum κ can be interpreted as a correlation length for the field or as a "bag radius." On the right side of Fig. 5, for the values of α shown, the frequencies W_K and Ω_K have been rescaled to align the minima. For a given α, the bands of points with different Λ interpolate a curve which illustrates the dispersion relation suggested by Gribov.[1] The plots also show how the location of the minimum changes when Λ and α are increased. For large α, however, these frequencies do not give a complete picture of the excited states, because there are also strong interactions between the gluons.

Figure 6 shows energies of excited 0^{++} states versus $n\alpha$ for $\Lambda=5$; note that the main n dependence is given by the Casimir operator. In this figure, as well as in Fig. 3 and in those which follow, the plotting symbols show the values of $n\alpha$ for which numerical calculations were made, and the connecting curves represent spline interpolations. Figure 6 shows that for $n\alpha\sim 1$, when the correlation length is similar to the size of the hypersphere, there is a transition to a regime in which there is a gap between excited states, as well as between excited states and the vacuum. In other words, there seems to be a transition from a perturbative regime, in which the quantization volume approximates part of a hadron's interior, to a confined regime in which the higher excited states are some approximation to a two-glueball continuum. The fact that the energies for different n are not coincident when $n\alpha$ is small is probably an artifact of our integration method; however, the region $n\alpha\gtrsim 1$ is not subject to this problem. The n dependence observed here originates in the n

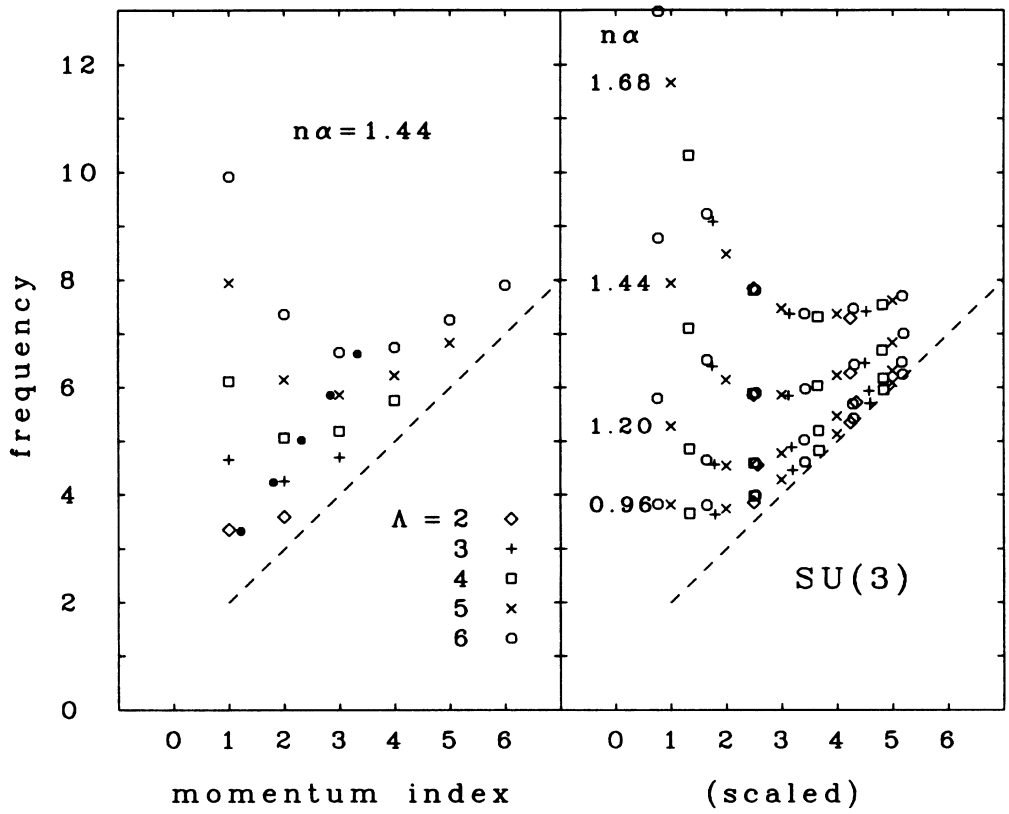

FIG. 5. Examples of effective gluon frequencies for SU(3).

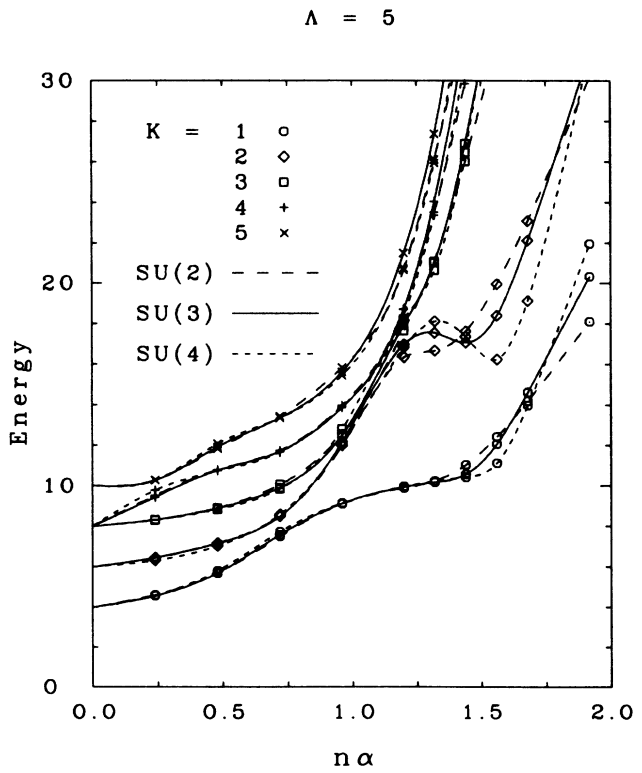

FIG. 6. Excitation energies for $\Lambda=5$. In this figure and in the remaining ones, the plotting symbols show the values of $n\alpha$ for which calculations were made, and the connecting curves are spline interpolations.

dependence of the U_K and Δ.

We find that the energy gap between the vacuum and the first excited state is about twice the characteristic gluon energy ω, for all the values of α, n, and Λ that we considered. As shown in Fig. 7, this enables us to plot all our results on a single graph. The second excited state is also shown. We see that, provided we stay away from weak- and super-strong-coupling regimes, there is a region where the Λ dependence of these ratios is not great. There are also smaller regions where the ratios to ω do not depend greatly on $n\alpha$, which determines the infrared scale. This value of $n\alpha$ is bigger for the second excited state, which is what one expects if the volume is to be big enough that the higher excited states can contain two separated glueballs. Of course, ω is only approximately interpretable as a physical quantity, so these ratios have only a qualitative significance. It is also possible that the scaling with respect to $n\alpha$ is distorted by hadron surface-energy corrections, as we mentioned earlier.

In Fig. 8 we show the relative contributions from different terms in the Hamiltonian to the energy difference between the vacuum and the first excited state. In this figure, C is the fractional contribution from the Coulomb term $\frac{1}{2}\epsilon^2$, while M is the fractional contribution from the magnetic energy $\frac{1}{2}B^2$. The fraction from the transverse electric energy, $\frac{1}{2}E^2$, is $1-C-M$. This is the largest single term. We see that in the confined regime, most of the energy difference between the first excited state and the vacuum is provided by the transverse electric field, while the contribution from the Coulomb energy is insignificant. This suggests that the glueball can be

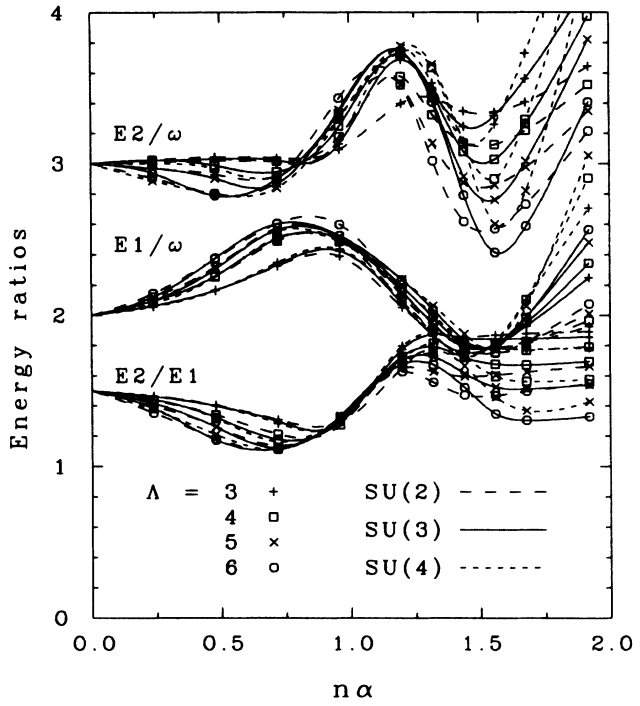

FIG. 7. Ratios of excitation energies.

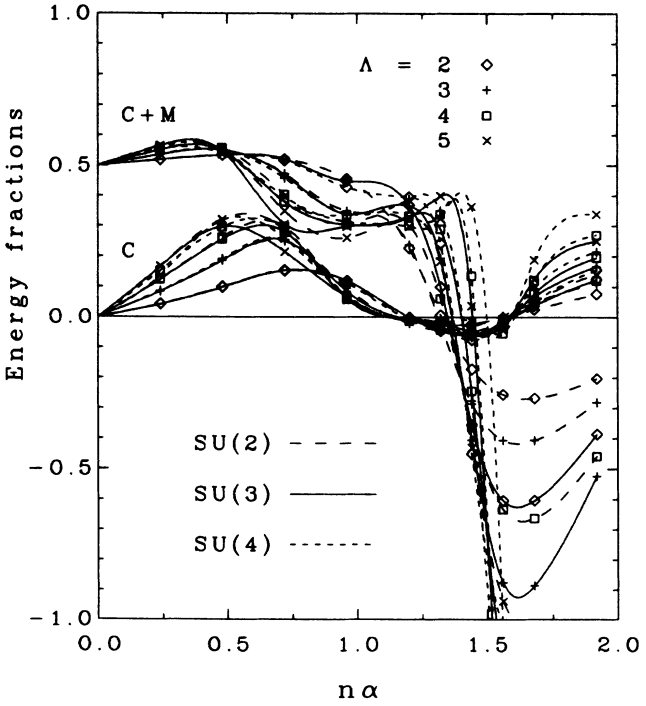

FIG. 8. Ratios of partial contributions to the first excitation energy, the "glueball mass." The fractional contribution of the Coulomb energy is C, the fractional contribution of the magnetic energy is M, and the fractional contribution of the transverse electric energy is $1-C-M$.

interpreted as a structure formed by endless lines of electric flux. The curve for $C+M$ has a somewhat irregular dependence on $n\alpha$. This may be a result of the fact that energy differences and partial energy contributions are often given less accurately than total energies, when a variational approach is used. It may also be, in part, a hadron surface-energy effect.

As a consequence of the well-known antiscreening effect of a Yang-Mills field, the "interior charge" σ should be smaller than the associated "exterior charge," which with our normalizations can be taken to be $\Gamma\nabla\cdot\epsilon$, or Φ. In Fig. 9 we show how the ratio of energies $I/E\equiv\langle\sigma^2\rangle/\langle\epsilon^2\rangle$ is decreased as α is increased. To examine properties of the longitudinal propagator in more detail, we use the ϕ_K^{LK} defined in Eq. (6) in terms of the projection operators Π^K, and consider the Coulomb-energy term

$$C(K,L)=\langle\sigma\Pi^K\Delta^{-1}\Pi^L\Delta^{-1}\Pi^K\sigma\rangle\ , \tag{18}$$

which exhibits the momentum correlation between the interior and exterior charges. We find that $C(K,L)$ can be represented as the sum of a Kronecker δ term $c(K)\delta_{KL}$ and a remaining "diffuse" term $d(K,L)$ in which K and L are essentially uncorrelated. The ratio of the diffuse part of the energy to the total Coulomb energy, $D/E\equiv\sum d(K,L)/\sum C(K,L)$, is also plotted in Fig. 9, and it is seen to also have a universal behavior.

In summary, our calculations support the idea that the characteristic dielectric properties of the QCD vacuum arise directly from properties of the electrical terms in the Hamiltonian, through the matrix Δ and from F. Even though the electric energy controls the dynamical behavior, large negative contributions to the electrical energy from the determinant F make $\langle B^2\rangle>\langle E^2+\epsilon^2\rangle$. A contrasting idea is that the dielectric properties of the

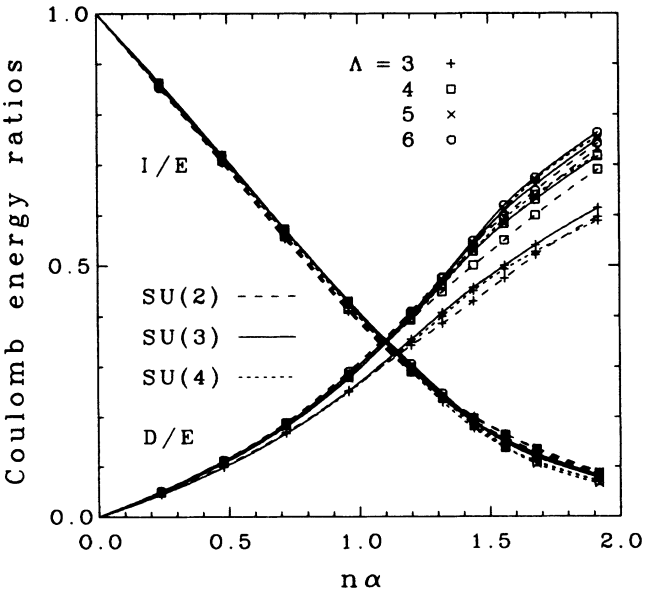

FIG. 9. The internal/external charges (normalized to give the energies) and the ratio of the diffuse component to the total external charge.

QCD vacuum arise more indirectly, from some other aspect of the theory. It has been suggested that there is an instability in the magnetic sector,[10,11,13] and that this leads to a state with very strong magnetic fields which might bring about a transition to a state in which electric flux lines would be compressed. However, there is no sign of magnetic instability in our calculations. Rather, the long-wavelength components of the Abelian part of the magnetic field are much weaker than in a free-field theory. Much of the phenomenology suggested by use of a dual potential as a mean field[7–9] nevertheless seems to be compatible with our conclusions about the behavior of the electric field, even though one of the ideas which had provided a motivation for these models is contradicted. Although we did not find any instability within the physical sector of QCD, it is possible to interpret the existence of null eigenvalues of Δ and the existence of the Gribov horizon as arising from an instability in the ghost sector.

In our SEA, as given by Eq. (13), we do not have a good estimate for the non-Abelian contribution to the total magnetic energy in the confined regime, or for how this energy might be apportioned among different wavelengths. Note that in constructing the SEA we used free-field energies in the internal loops, in order to have a simple, fixed expression for the Hamiltonian. If we were to use the effective frequencies given by Eq. (17) instead, the contributions would be reduced, especially the contributions to the attractive term. A more detailed variational study of these and other non-Abelian magnetic effects is projected.

Our nonperturbative numerical calculations have helped to clarify the mechanism for confinement of gluons in QCD. However, there are many questions which we have not yet investigated. We must examine excited states which have other quantum numbers, and include quarks. There are also many fundamental questions about Lorentz and gauge invariance which still need to be addressed.

ACKNOWLEDGMENTS

This work was supported by the U.S. Department of Energy under Contract No. DE-AC02-76ER-03066. Support for computation on the Cray X-MP/48 at the Pittsburgh Supercomputing Center has been provided by the NSF through Grants Nos. PH-8610729 and PSCA-195, and by grants from Cray Research, Inc. We thank J. Mahdavi for assistance with programming.

[1]V. N. Gribov, Nucl. Phys. **B139**, 1 (1978).
[2]R. E. Cutkosky, Phys. Rev. Lett. **51**, 538 (1983); **51**, 1603(E) (1983); Phys. Rev. D **30**, 447 (1984); Nucl. Phys. **B268**, 209 (1986).
[3]R. E. Cutkosky, Phys. Lett. B **194**, 91 (1987).
[4]D. Schütte, Phys. Rev. D **31**, 810 (1985); B. Faber, H. Nguyen-Quang, and D. Schütte, *ibid.* **34**, 1157 (1986); D. Schütte, Bonn Report No. TK 87 06 (unpublished).
[5]A. R. Swift and J. L. Morrero Rodriguez, Phys. Rev. D **29**, 1823 (1983); **31**, 917 (1985).
[6]N. H. Christ and T. D. Lee, Phys. Rev. D **22**, 939 (1980).
[7]S. Mandelstam, Phys. Rev. D **19**, 2391 (1979).
[8]V. P. Nair and C. Rosenzwieg, Phys. Lett. **134B**, 450 (1984).
[9]M. Baker, J. S. Ball, and F. Zachariasen, Phys. Rev. D **31**, 2575 (1985); **34**, 3894 (1986); M. Baker *et al.*, *ibid.* **33**, 1415 (1986).
[10]G. K. Savvidy, Phys. Lett. **71B**, 133 (1977); S. G. Matinyan and G. K. Savvidy, Nucl. Phys. **B134**, 539 (1978).
[11]N. K. Nielsen and P. Olesen, Nucl. Phys. **B144**, 376 (1978).
[12]S. Mandelstam, Phys. Rev. D **20**, 3223 (1979).
[13]M. Consoli and G. Preparata, Phys. Lett. **154B**, 411 (1985); L. Cosmai and G. Preparata, Phys. Rev. Lett. **57**, 2613 (1986).
[14]Jiang Liu and R. E. Cutkosky, Nucl. Phys. **B261**, 228 (1985).
[15]R. E. Cutkosky and K. C. Wang, Czech. J. Phys. B (to be published).
[16]R. E. Cutkosky, J. Math. Phys. **25**, 939 (1984).
[17]K. C. Wang and R. E. Cutkosky, Phys. Rev. D **36**, 3825 (1987).
[18]J. L. Balduz, R. E. Cutkosky, and W. Tsao, Nucl. Phys. **B261**, 239 (1985).
[19]S. Nojiri, Z. Phys. C **22**, 245 (1984).